

Dissociation of protonated oxalic acid $[\text{HOOC-C}(\text{OH})_2]^+$ into $\text{H}_3\text{O}^+ + \text{CO} + \text{CO}_2$: An experimental and CBS-QB3 computational study

Henri K. Ervasti^a, Richard Lee^b, Peter C. Burgers^c, Paul J.A. Ruttink^{a,*}, Johan K. Terlouw^b

^a Theoretical Chemistry Group, Department of Chemistry, University of Utrecht, 3584 CH Utrecht, The Netherlands

^b Department of Chemistry, McMaster University, 1280 Main St. W., Hamilton, Ont., Canada L8S 4M1

^c Laboratory for Neuro-Oncology, Department of Neurology, Erasmus MC, P.O. Box 1738, 3000 DR Rotterdam, The Netherlands

Received 31 October 2005; received in revised form 15 December 2005; accepted 20 December 2005

Available online 19 January 2006

In memory of Professor Chava Lifshitz, whom we remember as an excellent scientist and superb teacher and lecturer.

Abstract

The predominant dissociation process observed for metastable protonated oxalic acid ions $\text{HOOC-C}(\text{OH})_2^+$ (generated by self-protonation) leads to $\text{H}_3\text{O}^+ + \text{CO} + \text{CO}_2$. We have traced the mechanism of this intriguing reaction using the CBS-QB3 model chemistry. Our calculations show that a unique ter-body complex, $\text{O}=\text{C}=\text{O} \cdots \text{H}_3\text{O}^+ \cdots \text{CO}$, plays a key role in the rearrangement process. This complex can also dissociate to the proton bound dimers $[\text{H}_2\text{O} \cdots \text{H} \cdots \text{O}=\text{C}=\text{O}]^+$ and $[\text{H}_2\text{O} \cdots \text{H} \cdots \text{CO}]^+$ which are minor processes observed in the metastable ion mass spectrum. A further minor process leads to the proton bound dimer $\text{O}=\text{C}=\text{O} \cdots \text{H}^+ \cdots \text{CO}$ which is formed by water extrusion from the ter-body complex. Arguments are provided that the ter-body complex is also generated in the ion source by the collision encounter between neutral and ionized oxalic acid.

© 2005 Elsevier B.V. All rights reserved.

Keywords: Ab initio calculations; Proton transport catalysis; Unimolecular dissociation; Ter-body complex; Dimer radical cation

1. Introduction

The unimolecular dissociation paths of neutral oxalic acid, HOOC-COOH , have been examined previously by different experimental techniques [1a–c] and by various computational methods [1b–d]. The experimental studies have shown that ultraviolet photolysis and infrared multiphoton absorption lead to the following products: H_2O , CO , CO_2 and HCOOH , although their relative abundances vary considerably.

In an early computational study Kakumoto et al. [1b] calculated, at the Hartree-Fock (HF) level of theory and by using the 3–21G and 4–31G basis sets, the barrier heights associated with the unimolecular dissociation of oxalic acid. The lowest energy path corresponded to the formation of $\text{H}_2\text{O} + \text{CO} + \text{CO}_2$ with a relatively low barrier of 24 kcal mol^{-1} , whereas the barrier for the formation of $\text{CO}_2 + \text{HCOOH}$ was found to be significantly

higher, 67 kcal mol^{-1} . The barrier to form $\text{C}(\text{OH})_2$, dihydroxycarbene, which could act as an intermediate for formation of HCOOH and of $\text{H}_2\text{O} + \text{CO}$, was found to be 37 kcal mol^{-1} . A more recent theoretical study [1d] confirmed the earlier finding that formation of $\text{H}_2\text{O} + \text{CO} + \text{CO}_2$ is energetically the most favorable reaction, with a barrier of 42 kcal mol^{-1} . The barrier for the formation of $\text{HCOOH} + \text{CO}_2$ was found to be 62 kcal mol^{-1} .

Kinetic studies by Kakumoto et al. [1b] and by Higgins et al. [1d] support the finding from theory that formation $\text{H}_2\text{O} + \text{CO}_2 + \text{CO}$ is the favored unimolecular processes although Higgins et al. [1d] propose that a bimolecular process, rather than a unimolecular process, leads to HCOOH and CO , which would be kinetically more favorable than the unimolecular process.

Experimental and theoretical studies of oxalic acid ions are scarce. Ionized oxalic acid has been used to generate ionized dihydroxycarbene, $\text{C}(\text{OH})_2^{\bullet+}$ via loss of CO_2 [2]. A computational study has appeared [1e] dealing with oxalic acid anions and dianions, but no cations were studied.

* Corresponding author. Tel.: +31 302532734; fax: +31 302537504.

E-mail address: p.j.a.ruttink@chem.uu.nl (P.J.A. Ruttink).

Here, we investigate the unimolecular rearrangement and dissociation pathways of protonated oxalic acid. Interestingly, we observe that its major dissociation products ($\text{H}_3\text{O}^+ + \text{CO}_2 + \text{CO}$) are analogous to those ($\text{H}_2\text{O} + \text{CO}_2 + \text{CO}$) observed for the unimolecular dissociation of oxalic acid itself; note that of these products H_2O has the highest proton affinity. Using the CBS-QB3 model chemistry, a pathway was traced where the key intermediate is the ter-body complex $\text{O}=\text{C}=\text{O}\cdots\text{H}_3\text{O}^+\cdots\text{CO}$, which could also be viewed as a hydronium bound dimer. It is proposed that this ter-body complex is also generated in a collision encounter between ionized and neutral oxalic acid.

2. Experimental and theoretical methods

The experiments were performed with the VG analytical ZAB-R mass spectrometer of BEE geometry (B, magnet; E, electric sector) [3] using an electron ionization source at an accelerating voltage of 8 kV. Metastable ion (MI) mass spectra were recorded in the second field free region (2ffr). The CID mass spectra of the 2ffr metastable peaks were obtained in the 3ffr using O_2 as collision gas (Transmittance, $T=70\%$). All spectra were recorded using a PC-based data system developed by Mommers Technologies Inc. (Ottawa).

It is difficult to introduce oxalic acid into the ion source at controlled low pressures. When a probe tube containing anhydrous oxalic acid is introduced into the ion source, the pressure rapidly rises to $1\text{--}3 \times 10^{-5}$ Torr. At these pressures self-protonation is complete, i.e., there is no signal for ionized oxalic acid. We attempted to protonate oxalic acid by other means, but we could not eliminate the contribution of self-protonation (see Section 3).

The computations were performed using GAMESS UK [4] and Gaussian 98 [5] program packages. Initial optimizations of the molecules were obtained at DFT/B3LYP level of theory, after which CBS-QB3 model chemistry [6] implemented in the Gaussian 98 program package was used to obtain accurate complete basis set (CBS)-extrapolated values for the energy. From these accurate energies the values of the heat of formation at room temperature for each species was calculated using Radom's temperature correction method [7]. Spin contaminations were within acceptable range. The resulting total energies and enthalpies of formation for minima and connecting transition states (TS) in the protonated oxalic acid system are presented in Tables 1 and 2. Fig. 1 displays the optimized geometries for the principal species and Fig. 2 shows our derived potential energy surface (PES) for the rearrangement/dissociation processes of protonated oxalic acid. The complete set of computational results is available from the authors upon request.

3. Results and discussion

3.1. Structure, energy and stability of protonated oxalic acid

The most favorable protonation site of gaseous organic acids, $\text{RC}(=\text{O})\text{OH}$, is at the $\text{C}(=\text{O})$ oxygen atom to produce the carbe-

nium ion $\text{R}-\text{C}^+(\text{OH})_2$ [8]. In these ions the two powerful electron donating OH groups stabilize the positive charge by resonance. Depending on its nature, the substituent R may or may not lead to further stabilization.

In line with the above, our calculations show that for oxalic acid too the most favorable protonation site is at one of the carbonyl groups. Several conformers exist for the ground state, i.e., **1a1–1a6** in Fig. 1. The lowest conformers are found with the CBS-QB3 method to be $11.2 \text{ kcal mol}^{-1}$ for structure **1a1**, and $11.3 \text{ kcal mol}^{-1}$ for structure **1a2**. Slightly higher, at $\Delta_f H = 14.1 \text{ kcal mol}^{-1}$, is structure **1a3** and clearly higher one can find structures **1a4**, **1a5**, and **1a6**, at 17.7, 21.6, and $29.6 \text{ kcal mol}^{-1}$, respectively. All the stationary points of **1a1–1a6** can be transformed into each other over moderate barriers of $\sim 15\text{--}21 \text{ kcal mol}^{-1}$ (Table 1). Protonation at one of the OH groups leads to even higher energy species, **1b1–1b3** and so these will be inaccessible by low-energy protonation experiments. However, one of these structures, i.e., **1b3**, plays a crucial role in the dissociation of **1a1**.

Collision mass spectrometry based experiments lend support for structure $\text{HOOC}-\text{C}^+(\text{OH})_2$ formed by self-protonation. The CID mass spectrum, see Fig. 3(b), shows two intense peaks at m/z 45 and 46. These peaks, it is proposed, arise from the simple bond cleavages, **1a1** \rightarrow $\text{COOH}^+ + \text{C}(\text{OH})_2$ and **1a1** \rightarrow $\text{COOH}^\bullet + \text{C}(\text{OH})_2^{\bullet+}$. The calculated threshold energies of these processes are 93 and $115 \text{ kcal mol}^{-1}$, respectively, see Table 2 and so the signal at m/z 45 should be more abundant. From Fig. 3(b) it can be seen that the peaks at m/z 45 and 46 are of almost equal height, but the signal at m/z 45 is significantly broader making it the more abundant one. The peaks at m/z 29 and 19 correspond to consecutive dissociations of m/z 45 and 46 (part or all of m/z 19 may also be of metastable origin, see below). Minor peaks at m/z 74 and 56 can also be attributed to structure $\text{HOOC}-\text{C}^+(\text{OH})_2$ where loss of OH^\bullet may lead to ionized dihydroxycarbene, $\text{O}=\text{C}=\text{C}(\text{OH})_2^{\bullet+}$, m/z 74, which then loses H_2O to produce $\text{O}=\text{C}=\text{C}=\text{O}^{\bullet+}$, m/z 56 ($\text{O}=\text{C}=\text{C}(\text{OH})_2^{\bullet+} + \text{OH}^\bullet$ lies at $126 \text{ kcal mol}^{-1}$ (from $\Delta_f H [\text{O}=\text{C}=\text{C}(\text{OH})_2^{\bullet+}] = 117 \text{ kcal mol}^{-1}$, CBS-QB3, this work and $\Delta_f H [\text{OH}^\bullet] = 9 \text{ kcal mol}^{-1}$ [8]) and so this process can only be observed upon collisional excitation).

The activation energy for the cleavage of lowest energy requirement is 82 kcal mol^{-1} (see Fig. 2), which is similar in magnitude to bond dissociation energies of neutral molecules and so protonated oxalic acid would appear to be very stable. However, far below this dissociation limit, **1a1** can undergo an intriguing rearrangement by step-wise or synchronous decarbonylation and decarboxylation.

3.2. Rearrangement and dissociation reactions of protonated oxalic acid

The MI mass spectrum of **1a1** is shown in Fig. 3(a). The most important peak is at m/z 19 (H_3O^+) corresponding to the loss of CO and CO_2 . Minor signals are observed at m/z 63 (loss of CO), m/z 47 (loss of CO_2) and m/z 73 (loss of H_2O). The signals at

Table 1
Enthalpies of formation of protonated oxalic acid and isomers derived from CBS-QB3 calculations

Ions		E_{total} (0 K)	ZPE	ΔH_f° (0 K)	ΔH_f° (298 K)
(HO) ₂ C-COOH ⁺ [S]	1a₁	-378.16186	38.2	14.8	11.2
(HO) ₂ C-COOH ⁺ [W]	1a₂	-378.16176	38.3	14.8	11.3
(HO) ₂ C-COOH ⁺ [S]	1a₃	-378.15723	38.1	17.7	14.1
(HO) ₂ C-COOH ⁺ [S]	1a₄	-378.15159	37.9	21.2	17.7
(HO) ₂ C-COOH ⁺ [U]	1a₅	-378.14544	37.8	25.1	21.6
(HO) ₂ C-COOH ⁺ [U]	1a₆	-378.13285	37.3	33.0	29.6
TS 1a₁-1a₂	Rotation	-378.13862	36.8	29.4	25.7
TS 1a₁-1a₅	Rotation	-378.13048	36.5	34.4	30.9
TS 1a₃-1a₅	Rotation	-378.12937	36.5	35.1	31.6
TS 1a₄-1a₁	Rotation	-378.14302	36.9	26.6	23.0
TS 1a₅-1a₆	Rotation	-378.12703	36.4	36.6	33.2
TS 1a₄-1a₆	Rotation	-378.11796	36.1	42.3	39.0
H ₂ O-C(=O)COOH ⁺	1b₁	-378.12420	36.1	38.4	35.3
H ₂ O-C(=O)COOH ⁺	1b₃	-378.12652	35.9	37.0	34.2
[O=C=O...HOH(H)...C=O] ⁺	1c₁	-378.19180	34.1	-4.0	-5.7 [-4.7]
[HO-C(=O)...O(H)H...C=O] ⁺	1c₂	-378.13396	34.4	32.2	30.3
[O=C...H...O(H)-C(=O)OH] ⁺	1c₃	-378.14849	34.7	23.1	20.7
[O=C=O...H...O(H)-C(H)=O] ⁺	1d₁	-378.16585	34.9	12.2	10.0 [11.0]
[O=C=O...H...O(H)-C(H)=O] ⁺	1d₂	-378.16560	34.8	12.4	10.3
[O=C=O...H...O-C(H)-OH] ⁺	1d₃	-378.19586	36.9	-6.6	-9.2
[O=C=O...H-C(OH) ₂] ⁺	1d₄	-378.19737	36.9	-7.6	-10.2
(HO) ₃ C-C=O ⁺	1e	-378.17585	36.0	5.9	3.7
[O=C...H...O-C(OH) ₂] ⁺	1f	-378.18502	36.2	0.2	-2.5
(HO) ₂ C-O-C(H)=O ⁺	1g	-378.15797	36.0	17.9	14.1
[O=C=O...H...O(H)-C-OH] ⁺	1h	-378.10775	34.7	48.7	46.4
TS 1b₃-1c₁ (Fig. 2)		-378.11318	34.7	45.3	42.6
TS 1a₁-1e (Fig. 2)		-378.08623	35.4	62.2	58.7
TS 1c₁-1d₁ (Fig. 2)		-378.16149	32.3	15.0	13.4
TS 1d₂-1d₃ (Fig. 2)		-378.14591	34.7	24.7	21.7 [23.8]
TS 1d₁-1d₂ (Fig. 2)		-378.16086	34.6	15.4	12.9
TS 1a₂-1b₃ (Fig. 2)		-378.12456	35.2	38.1	34.5
TS 1c₃-1g (Fig. 5)		-378.14653	33.8	24.3	21.2
TS 1f-1g (Fig. 5)		-378.14563	34.9	24.9	22.1
TS 1c₂-1c₃ (Fig. 5)		-378.13306	33.7	32.8	30.4
TS 1c₁-1c₂ (Fig. 5)		-378.13502	33.8	32.0	29.5
TS 1a₄-1h		-378.09033	34.7	59.6	56.3
TS 1a₄-1d₄		-378.08291	35.0	64.3	61.4

Values in square brackets refer to CBS-APNO results.

m/z 29, 45, 46 and 56 are completely of collision origin resulting from the presence of residual collision gas. In the following we discuss the metastable losses of CO, CO₂, CO + CO₂ and of H₂O.

First we identify the CH₃O₂⁺ ions at m/z 47 and the CH₃O₃⁺ ions at m/z 63. In Fig. 4(a) and (b) are given the reference CID spectra of the m/z 47 CH₃O₂⁺ ions, to wit protonated formic acid, HC(OH)₂⁺ generated from ionized ethyl formate, and the proton bound dimer H₂O...H⁺...CO formed in a CI experiment of CO with a trace of water [9]. The latter CID spectrum is dominated by a narrow peak at m/z 19, whereas that for HC(OH)₂⁺ gives an intense peak at m/z 29. The CID spectrum of the CH₃O₂⁺ ions generated from metastable **1a₁** is shown in Fig. 4(c). Now we had already observed that in the MI mass spectrum of **1a₁** the metastable peak at m/z 47 is much weaker than the collision induced peak at m/z 46 and so the CID spectrum of m/z 47 will be heavily contaminated by contributions from C(OH)₂^{•+}. This

species gives signals at m/z 29, 28, 18, 17 and 12 in a ratio of 100:40:14:13:2 and so we can only use the narrow peak at m/z 19 to identify the CH₃O₂⁺ ions. Such a signal is compatible with the structure H₂O...H⁺...CO, where the proton will be more closely associated with the water molecule because the proton affinity (PA) of water is larger than that of CO [8]. However, we cannot exclude the possibility that some HC(OH)₂⁺ ions are co-generated. We have tried to separate the m/z 47 peak from the intense signal at m/z 46 by examining the MI spectrum of the fully D labeled ions DOOC-C(OD)₂⁺, where m/z 50 is separated from m/z 48. However, in this experiment we find that m/z 50 is now contaminated by DO-C-¹⁸OD^{•+} generated by losses of CO₂ from the oxalic acid-OD₂, ¹⁸O molecular ions.

In Fig. 4(d) and (e) are given the reference CID spectra of m/z 63 CH₃O₃⁺, namely protonated carbonic acid, C(OH)₃⁺, formed from ionized diethyl carbonate [10], and the proton bound dimer H₂O...H⁺...O=C=O generated by the dissociative ionization of

Table 2

Enthalpies of formation of dissociation products of protonated oxalic acid derived from CBS-QB3 calculations^a

Ions		E_{total} (0 K)	ZPE	ΔH_f° (0 K)	ΔH_f° (298 K)
$\text{H}_3\text{O}^+ + \text{CO} + \text{CO}_2$					21
H_3O^+		-76.59652	21.4	145.2	143.6
CO		-113.18197	3.1	-27.7	-26.9
CO_2		-188.37223	7.3	-95.8	-95.9
$\text{H}-\text{C}(\text{OH})_2^+ + \text{CO}_2$					1
$[\text{O}=\text{C}\cdots\text{H}\cdots\text{OH}_2]^+ + \text{CO}_2$					6
$\text{H}-\text{C}(\text{OH})_2^{+\text{b}}$	2a	-189.80656	29.0	99.9	97.2
$\text{H}-\text{C}(=\text{O})\text{OH}_2^+$	2b	-189.77544	26.5	119.5	117.5
$[\text{O}=\text{C}\cdots\text{H}\cdots\text{OH}_2]^+$	2c	-189.80110	25.7	103.4	101.7
$[\text{C}=\text{O}\cdots\text{H}\cdots\text{OH}_2]^+$	2d	-189.79193	25.7	109.1	107.8
$\text{HO}-\text{C}-\text{OH}_2^+$	2e	-189.71594	26.3	156.8	154.8
Fig. 5(b)	2a-CO	-303.00598	33.0	61.3	59.2
Fig. 5(b)	2b-CO	-302.97500	30.8	80.8	79.2
Fig. 5(b)	2b-CO'	-302.97453	31.0	81.1	79.4
Fig. 5(b)	2c-CO	-303.00040	30.2	64.8	63.6
TS 2a-CO – 2b-CO		-302.96963	30.8	84.1	81.6
TS 2b-CO – 2b-CO'		-302.96943	30.8	84.3	82.3
TS 2b-CO' – 2c-CO		-302.96824	28.4	85.0	84.1
$\text{C}(\text{OH})_3^+ + \text{CO}$					8
$[\text{O}=\text{C}=\text{O}\cdots\text{H}\cdots\text{OH}_2]^+ + \text{CO}$					6
$\text{C}(\text{OH})_3^{+\text{b}}$	3a	-264.98695	32.2	38.0	34.6
$\text{HO}-\text{C}(=\text{O})\text{OH}_2^+$	3b	-264.94565	30.6	63.9	61.0
$[\text{O}=\text{C}=\text{O}\cdots\text{H}\cdots\text{OH}_2]^+$	3c	-264.99197	29.6	34.8	32.7
TS 3a – 3b		-264.90297	28.4	90.7	87.3
TS 3b – 3c		-264.92845	29.1	71.0	68.3
$\text{HO}-\text{C}(=\text{O})\text{C}=\text{O}^+ + \text{H}_2\text{O}$					52
$[\text{O}=\text{C}=\text{O}\cdots\text{H}\cdots\text{C}=\text{O}]^+ + \text{H}_2\text{O}$					29
$\text{HO}-\text{C}(=\text{O})\text{C}=\text{O}^+$	4a	-301.76187	19.4	111.5	110.5
$[\text{O}=\text{C}=\text{O}\cdots\text{H}\cdots\text{C}=\text{O}]^+$	4b	-301.80091	17.5	87.4	87.1
H_2O		-76.33746	13.2	-57.5	-58.2
$\text{HO}-\text{C}=\text{O}^+$		-188.57461	13.3	142.5	141.8
$\text{H}-\text{C}=\text{O}^+$		-113.40509	10.2	197.6	197.5
$\text{HO}-\text{C}-\text{OH}^{*\text{+}}$ (W conformer)		-189.12578	20.4	161.9	160.3
$\text{HO}-\text{C}-\text{OH}$ (S conformer)		-189.45926	20.5	-47.4	-49.1
HOCO^\bullet		-188.87250	13.0	-44.5	-45.2
$(\text{HO})_2\text{C}=\text{O}^\text{b}$		-264.69558	24.5	-144.5	-146.9

^a E_{total} in Hartrees, all other values in kcal mol⁻¹, including the ZPE scaled by 0.99.^b Lowest energy conformer.

dihydroxyfumaric acid [10]. The latter spectrum is characterized by a narrow peak at m/z 19, H_3O^+ , as was also the case for $\text{H}_2\text{O}\cdots\text{H}^+\cdots\text{CO}$, see above. The CID spectrum of the CH_3O_3^+ ions generated from metastable **1a₁** ions is given in Fig. 4(f) and it can be seen that these ions are $\text{H}_2\text{O}\cdots\text{H}^+\cdots\text{O}=\text{C}=\text{O}$ to the exclusion of $\text{C}(\text{OH})_3^+$.

Thus, the following dissociations have been established:



According to our calculations the conformer **1a₂** ($\Delta_f H = 11.3$ kcal mol⁻¹) can rearrange without a barrier to the hydroxyl protonated form $\text{HOOC}-\text{C}(=\text{O})\text{OH}_2^+$, **1b₃**, which lies 35 kcal mol⁻¹ above **1a₂**; alternatively, see Table 1 and Fig. 2, we can start from **1a₁** ($\Delta_f H = 11.2$ kcal mol⁻¹)

which can then, via a barrier at 26 kcal mol⁻¹, rearrange to **1a₂**. The associated transition state (TS **1a₂-1b₃**) as well as **1b₃** are essentially planar. Next the H_2O moiety rotates to such an extent (TS **1b₃-1c₁**) that the carboxyl hydrogen can be transferred to the H_2O ionic part. This leads to collapse to the ter-body [11] complex $\text{O}=\text{C}=\text{O}\cdots\text{H}_3\text{O}^+\cdots\text{CO}$ (**1c₁**) which in fact is a double hydrogen bridged species and which can also be viewed as a hydronium bound dimer. Thus, after the second hydrogen shift, the C–C bond stretches and the incipient H_3O^+ ion inserts itself into this elongated C–C bond forming H-bonds with CO and CO_2 . This ter-body complex serves as the reacting configuration (RC) for reactions (1)–(3). It can be seen from Table 2 and Fig. 2 that the dissociation energies to produce H_3O^+ from $\text{H}_2\text{O}\cdots\text{H}^+\cdots\text{O}=\text{C}=\text{O}$ and $\text{H}_2\text{O}\cdots\text{H}^+\cdots\text{CO}$ are the same, 15 kcal mol⁻¹. This means that CO and CO_2 have the same hydronium ion affinity. Thus, energetically it makes no difference whether we associate H_3O^+ with CO or CO_2 and as

a consequence association with a second CO or CO₂ molecule, too, makes no difference. As can be seen from Fig. 2, a single complexation leads to a stabilization of 15 kcal mol⁻¹ and the second one to a further stabilization of 12 kcal mol⁻¹.

We note here that the barrier for formation of H₃O⁺ + CO + CO₂ is 32 kcal mol⁻¹, which is similar to the barrier found for formation of H₂O + CO + CO₂ for neutral oxalic acid, 24 [1b] or 42 kcal mol⁻¹ [1d] although the respective mechanisms are very different. Hence, protonation does not appear to accelerate decomposition of oxalic acid.

The ter-body complex **1c₁** may also lead to the loss of H₂O to produce the proton bound dimer O=C=O ··· H⁺ ··· CO (*m/z* 73). According to our calculations the O–H ··· C hydro-

gen in **1c₁** may move towards the C atom of CO and the H₂O molecule is then “extracted” from the complex to produce the TS (**1c₁**–**1d₁**) which can be considered as the proton bound dimer O=C=O ··· H⁺ ··· CO with an additional water molecule associated with the proton. This TS may generate the proton bound dimer O=C=O ··· H⁺ ··· O(H)–CH=O, **1d₁**, or it may shed H₂O to produce O=C=O ··· H⁺ ··· CO, *m/z* 73. This ion could fragment further to HCO⁺ + CO₂ (+H₂O) and this process has a threshold energy of 44 kcal mol⁻¹. Since the intensity ratio *m/z* 29:*m/z* 45 is the same in Fig. 3(a) and (b) we conclude that most of *m/z* 29 in the MI spectrum (Fig. 3(a)) is of collision induced origin. This leads to an important conclusion: the internal energy of metastable protonated oxalic acid cannot be much larger than

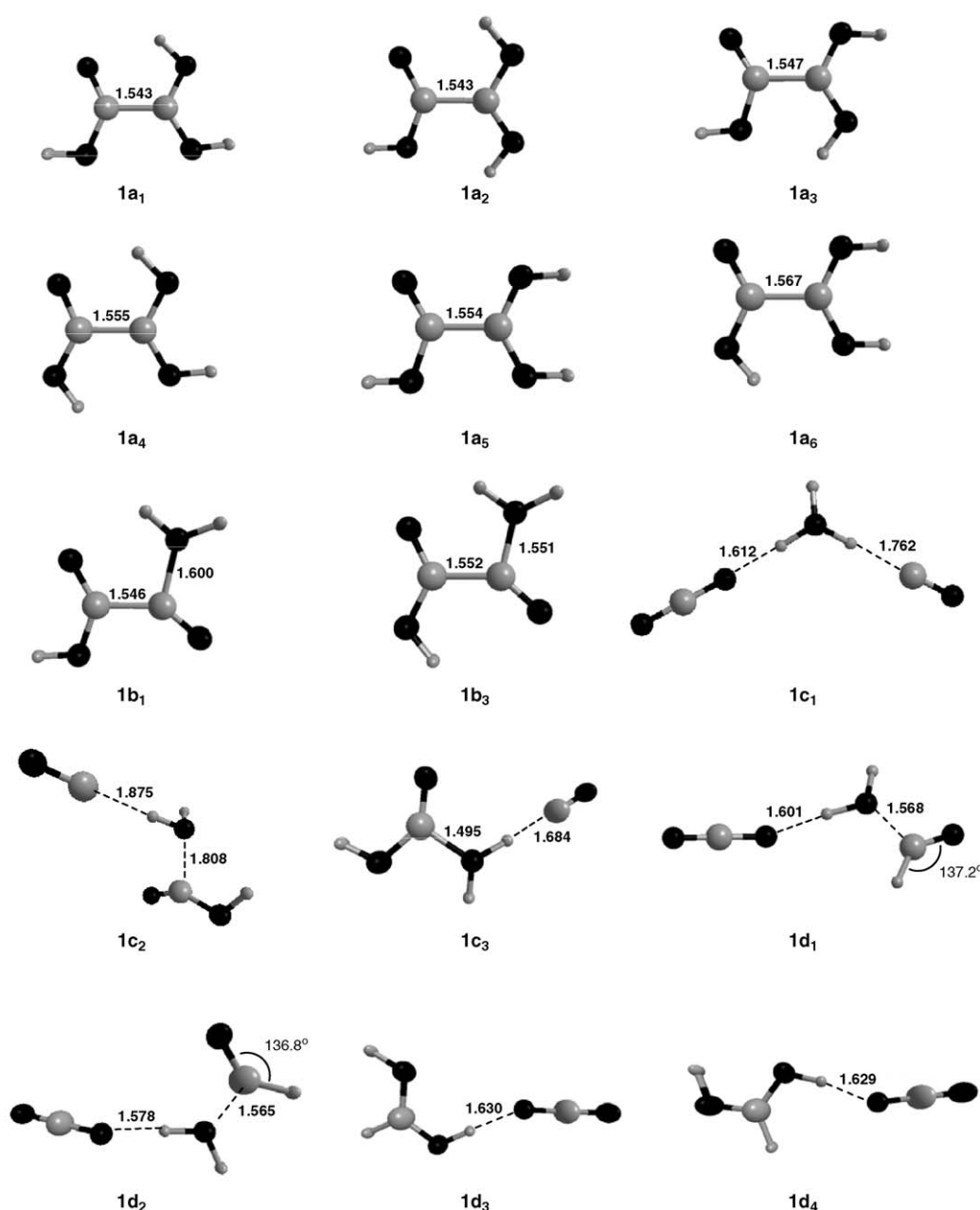


Fig. 1. The CBS-QB3 optimized geometries for protonated oxalic acid isomers and selected transition states.

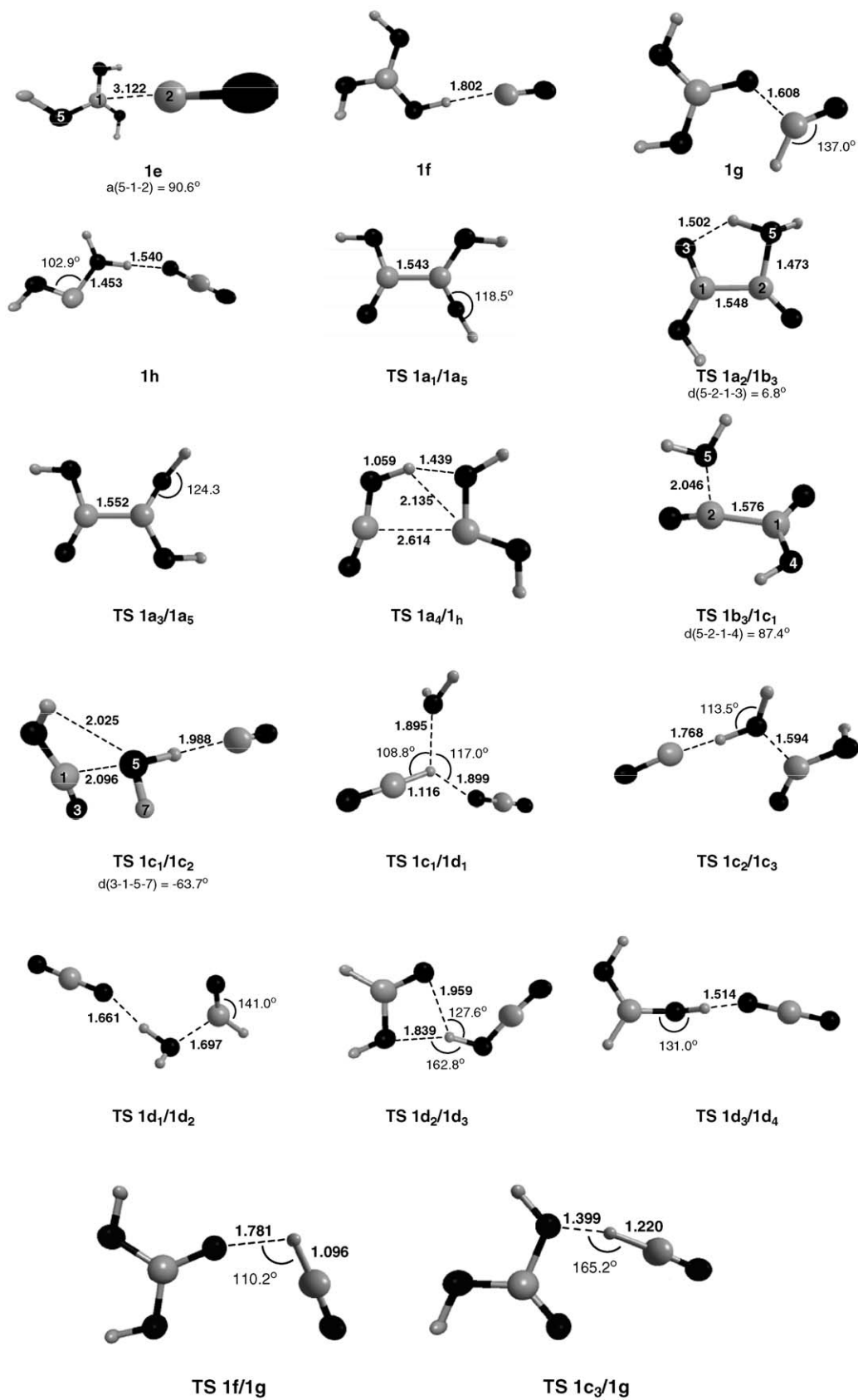


Fig. 1. (Continued).

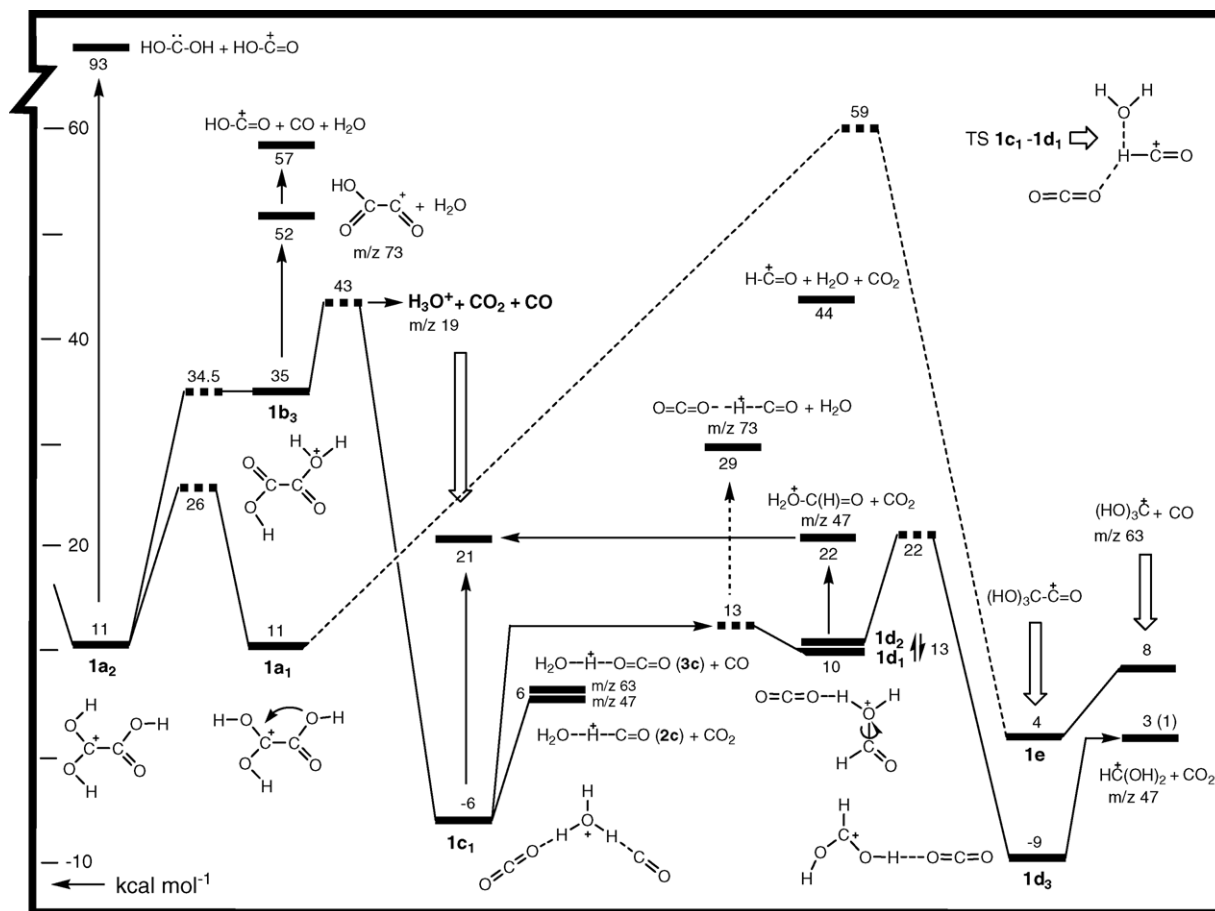


Fig. 2. Potential energy diagram derived from CBS-QB3 (298 K, Tables 1 and 2) calculations describing the dissociation chemistry of metastable protonated oxalic acid ions.

44 kcal mol⁻¹ which imposes an upper energy limit upon our theoretical calculations. Thus, certain mechanistic alternatives, how attractive they may be, can now be ruled out. For example, the barrier for a least-motion extrusion of CO from conformer **1a₁** to produce C(OH)₃⁺ from **1e** lies at 59 kcal mol⁻¹ (see Fig. 2) and so this process can be ruled out.

In the same vein, direct formation of HC(OH)₂⁺ by loss of CO₂ is also energetically prohibited: the transition state associated with the 1,3-H shift in the reaction sequence **1a₄** → **1d₄** → HC(OH)₂⁺ + CO₂ lies at 61 kcal mol⁻¹ (Table 2). Alternatively, a 1,4-H shift with a concomitant C–C cleavage in **1a₄** would yield ion **1h**, O=C=O ··· H–O⁺(H)–C–OH. This ion could rearrange into **1d₄**, O=C=O ··· H–C⁺(OH)₂, by proton transport catalysis, and then lose CO₂. However, the transition state for **1a₄** → **1h** lies at 56 kcal mol⁻¹, see Table 1, and so this process can also be ruled out.

Summarizing, our CBS-QB3 calculations can rationalize the formation of the dissociation products (H₃O⁺, H₂O ··· H⁺ ··· CO, H₂O ··· H⁺ ··· O=C=O and O=C=O ··· H⁺ ··· CO) of protonated oxalic acid in terms of the intermediary of the ter-body complex O=C=O ··· H₃O⁺ ··· CO. However, some disconcerting questions remain, to wit:

1. We can rationalize the formation of the proton bound dimers H₂O ··· H⁺ ··· CO and H₂O ··· H⁺ ··· O=C=O; we can also

rationalize that the conventional species HC(OH)₂⁺ and C(OH)₃⁺ are not formed directly from **1a**. However, can we also rule out the formation of HC(OH)₂⁺ and C(OH)₃⁺ via other pathways, for example, via further isomerization of the molecular ion or of the product ions?

2. The products H₂O ··· H⁺ ··· CO and H₂O ··· H⁺ ··· O=C=O are formed with a large amount of excess energy (37 kcal mol⁻¹, see Fig. 2) and so the question arises as to why these proton bound dimers (or at least part of them) remain intact. Also, what is the reason that two iso-energetic products (formation of *m/z* 47 and 63) give markedly different ion yields in the MI spectrum? And lastly, formation of *m/z* 73 needs 23 kcal mol⁻¹ more energy than generation of *m/z* 47, so why are the two corresponding metastable peaks of nearly equal intensity?

3.3. Transformation of O=C=O ··· H₃O⁺ ··· C=O into O=C=O ··· H–O–CHOH⁺

With respect to the first question, we have already established that the ter-body complex **1c₁** can rearrange into O=C=O ··· H⁺ ··· O(H)–CH=O, **1d₁**, see Fig. 2. This species can rearrange via a low barrier to its conformer **1d₂**. In this species the CO₂ molecule can accept the proton and after passing TS (**1d₂**–**1d₃**) at 22 kcal mol⁻¹, the proton is donated back to the

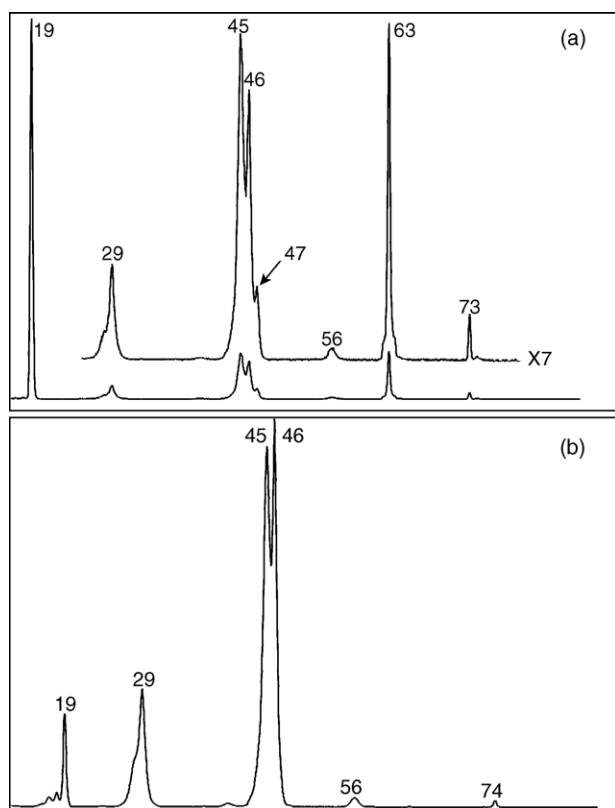


Fig. 3. MI and CID mass spectra of protonated oxalic acid, item (a) and (b), respectively.

carbonyl oxygen atom of the incipient HO–CH=O molecule to produce the very stable complex $\text{HC}(\text{OH})_2^+ \cdots \text{O}=\text{C}=\text{O}$ (**1d₃**) which can then shed CO_2 to produce $\text{HC}(\text{OH})_2^+$. This constitutes an example of proton-transport catalysis (PTC [12]), by now a well-established process. In a recent publication [13] on the isomerization/dissociation reactions of metastable $\text{HC}(\text{OH})_2^+$ ions, **2a**, it was concluded that these ions can rearrange via a 1,3-H shift to the ion–dipole complex $\text{H}-\text{C}^+(\text{=O}) \cdots \text{OH}_2$, **2b**, which is a transient species only and which collapses to the complex $\text{O}=\text{C} \cdots \text{H}^+ \cdots \text{OH}_2$, **2c**. For the reverse reaction **2b** → **2a** the barrier was found to be 30 kcal mol^{-1} . When we complex **2a** with CO_2 as in **1d₂** the barrier is reduced to 12 kcal mol^{-1} , see Fig. 2 (TS **1d₂**–**1d₃**) and so CO_2 does catalyze the reaction to some extent by PTC. This barrier lies far beneath the energy for formation of **1d₂** from protonated oxalic acid, so that energetically PTC may well occur. However, as discussed above, we cannot conclude from our experimental data whether or not this process actually occurs to some extent. The reason that the CO_2 assisted isomerization (**2b** → **2a**) still has a sizeable barrier lies in the low PA of CO_2 ($129 \text{ kcal mol}^{-1}$) compared to the PAs of $\text{H}-\text{C}(\text{=O})-\text{OH}$ at =O ($179 \text{ kcal mol}^{-1}$ [8]) and at $-\text{OH}$ ($159 \text{ kcal mol}^{-1}$, from Table 2). Indeed, when we complex **2b** with a species having a higher PA, e.g., CO (PA = $142 \text{ kcal mol}^{-1}$, i.e., more in line with Radom's PA criterion [14]) we calculate that the barrier is reduced to a mere 2 kcal mol^{-1} .

3.4. Transformation of $\text{O}=\text{C}=\text{O} \cdots \text{H}_3\text{O}^+ \cdots \text{C}=\text{O}$ in to $\text{O}=\text{C} \cdots \text{H}-\text{O}-\text{C}(\text{OH})_2^+$

Experimentally, the situation is much clearer for the loss of CO, where the sole product is $\text{H}_2\text{O} \cdots \text{H}^+ \cdots \text{O}=\text{C}=\text{O}$, **3c**, to the exclusion of $\text{C}(\text{OH})_3^+$, **3a₁**. We have traced a low energy pathway where CO catalyzes the transformation **3c** → **3a₁** and the results of our calculations are shown in Fig. 5. In Fig. 5(a) is shown the potential energy surface (PES) for rearrangement/dissociation processes of the solitary ions $\text{H}_2\text{O} \cdots \text{H}^+ \cdots \text{O}=\text{C}=\text{O}$ and $\text{C}(\text{OH})_3^+$. Starting from **3a₁**, a 1,3-H shift requires 52 kcal mol^{-1} to produce the ion–dipole complex $\text{HOC}^+(\text{=O}) \cdots \text{OH}_2$, **3b**, which can either lose water as indicated, or it can shift the proton from HOCO^+ to H_2O to produce **3c** which can then dissociate. However, when we start from low energy ions **3c** isomerization into **3a₁** will not take effect because the barrier (52 kcal mol^{-1}) is much larger than the threshold for dissociation into $\text{H}_3\text{O}^+ + \text{CO}_2$. It is also clear that even ions **3c** having internal energies of $37\text{--}39 \text{ kcal mol}^{-1}$, i.e., those formed from protonated oxalic acid as depicted in Fig. 2 cannot isomerize into **3a₁**.

How does the situation change when the proton bound dimer **3c** is complexed with CO, as in **1c₁**? Here, see Fig. 5(b), we find that isomerization of **1c₁** into **1c₃**, the CO complexed analog of **3b**, requires about as much energy as rearrangement for the isolated ion. However, the next steps leading to **1f**, the analogue of **3a**, require substantially less energy when the ion is associated with CO. In this rearrangement of **1c₃** → **1f** the CO molecule attracts the proton, and then the C atom of the incipient HCO^\bullet radical forms a covalent bond with the keto oxygen atom (as indicated by the arrow) to form the carbenium ion **1g**. The next step is analogous to decarbonylation of ionized methyl formate [15]: the O–C bond stretches and the proton is inserted into this stretched bond to form the complex **1f** which could then dissociate. The reaction **1c₃** → **1f** could be called proton-transport catalysis, but it proceeds via a covalently bonded carbenium ion. The activation energy for the rearrangement **1c₁** → **1f** is 36 kcal mol^{-1} , compared to 54 kcal mol^{-1} for the solitary ions and considering that ions **1c₁** have an internal energy of $49\text{--}51 \text{ kcal mol}^{-1}$, formation of $\text{C}(\text{OH})_3^+$ is energetically feasible. In Fig. 2, the barrier for the above CO assisted reaction lies at 30 kcal mol^{-1} , at the energy level for formation of m/z 73. Experimentally it is found that m/z 73 is formed whereas $\text{C}(\text{OH})_3^+$ is not. We propose that kinetic factors rule against the formation of $\text{C}(\text{OH})_3^+$: the internal energy available to **1c₁** is so large that the ion will preferentially undergo simple cleavage reactions rather than complicated rearrangement processes.

3.5. Formation of $\text{O}=\text{C}=\text{O} \cdots \text{H}_3\text{O}^+ \cdots \text{C}=\text{O}$ from the oxalic acid dimer radical cation

The second problem concerns the observation that at least part of the **2c** and **3c** ions having large internal energies ($37\text{--}39 \text{ kcal mol}^{-1}$) remain intact. The excess energy is $22\text{--}24 \text{ kcal mol}^{-1}$ which should be more than sufficient to completely dissociate these complexes within the metastable time frame. The origin of the problem may lie in the method of ion

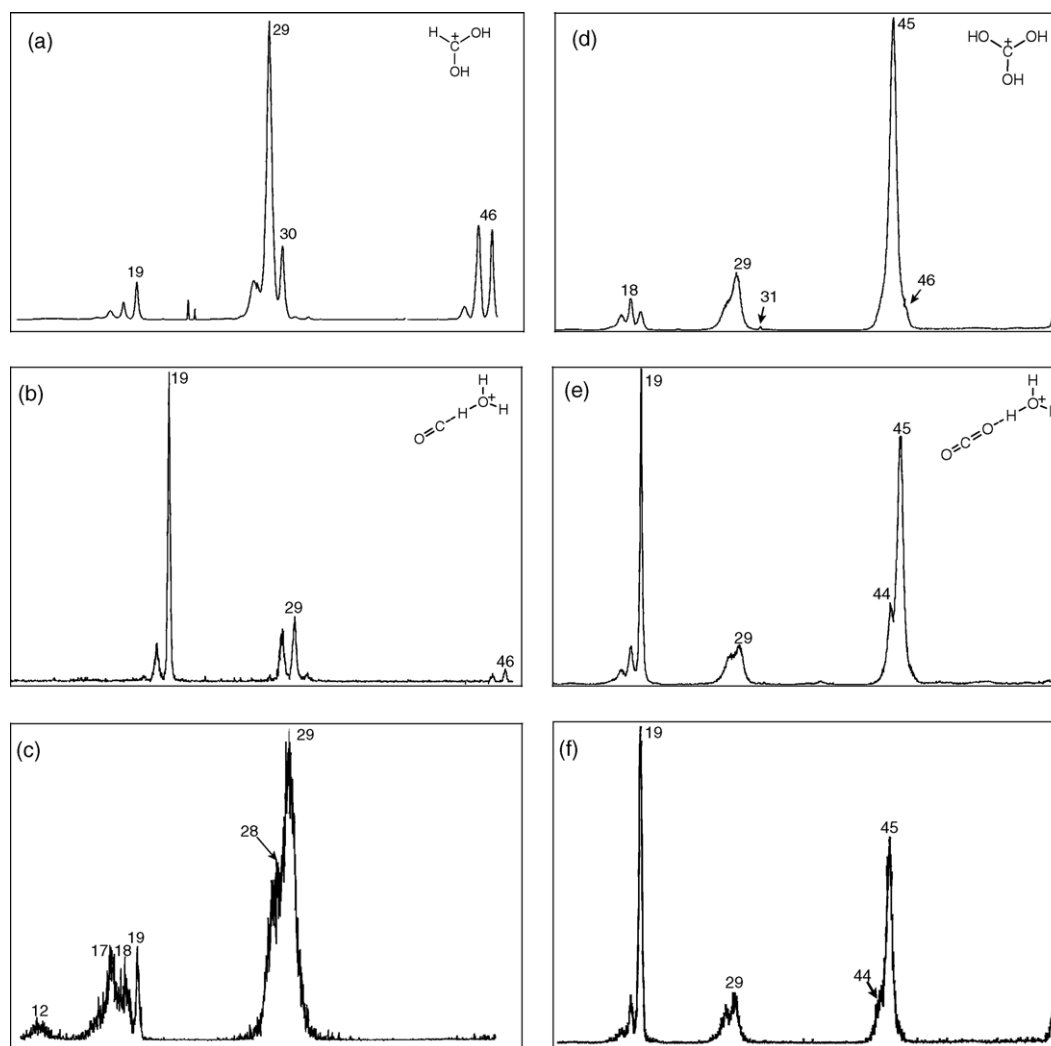
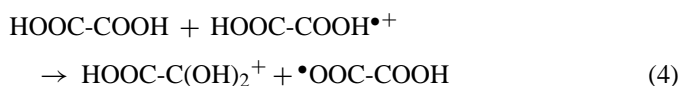


Fig. 4. CID mass spectra of m/z 47 CH_3O_2^+ ions (items a–c) and m/z 63 CH_3O_3^+ ions (items d–f): (a) protonated formic acid $\text{HC}(\text{OH})_2^+$; (b) proton-bound dimer $[\text{H}_2\text{O}-\text{H}-\text{CO}]^+$; (c) m/z 47 CH_3O_2^+ ions generated from the unimolecular decomposition of protonated oxalic acid ions; (d) $\text{C}(\text{OH})_3^+$; (e) proton bound dimer $[\text{H}_2\text{O}-\text{H}-\text{OCO}]^+$; (f) m/z 63 CH_3O_3^+ ions generated from the unimolecular decomposition of protonated oxalic acid ions.

preparation. As mentioned in Section 2 protonated oxalic acid was produced by self-protonation, putatively by the following reaction:



According to our ab initio calculations the PAs of oxalic acid and of the radical $\bullet\text{OOC}-\text{COOH}$ are similar and so the proton can easily shift from the radical cation to the neutral molecule. Next an interesting phenomenon may occur: our calculations indicate that the C–C bond in the radical $\bullet\text{OOC}-\text{COOH}$ is very weak so that the radical may dissociate exothermically to $\text{HOCO}^\bullet + \text{CO}_2$. That is to say the initial hydrogen bridged radical cation $\text{HOOC}-\text{C}(\text{=O})-\text{O}^\bullet \cdots \text{H}^+ \cdots \text{O}=\text{C}(\text{OH})-\text{COOH}$, see also Fig. 6, loses COOH^\bullet to produce protonated oxalic acid complexed with CO_2 . Next, the ter-body complex $\mathbf{1c}_1$ is generated by the same mechanism as shown in Fig. 2 for solitary protonated oxalic acid but now with CO_2 as a spectator molecule. That CO_2

is no more than a spectator follows from the observation that the activation energies for the isolated reaction and for reaction with CO_2 are equal (32 kcal mol^{-1}). The overall reaction depicted in Fig. 6 is exothermic by $41.5 \text{ kcal mol}^{-1}$ and so the ter-body complex thus formed is expected to dissociate. However, this ion-molecule reaction takes place in the source under chemical ionization conditions where the ter-body complex can be collisionally stabilized. Hence, it is entirely possible that in the ion source ions $\mathbf{1c}_1$ are already present in admixture with solitary protonated oxalic acid ions. Such $\mathbf{1c}_1$ ions we argue are the precursors for formation of m/z 47 and 63 as observed in the MI mass spectrum, whereas protonated oxalic acid would dissociate only to H_3O^+ . Can we prove this hypothesis? We could for example try to protonate oxalic acid by other means than by self-protonation. However, as mentioned in Section 2, it proved very hard to reduce the amount of self-protonation in favour of protonation by another agent (e.g., H_2O). Another attempt would be to purify the m/z 91-ion beam by a neutralization-reionization experiment followed by MI analysis of the survivors. The idea

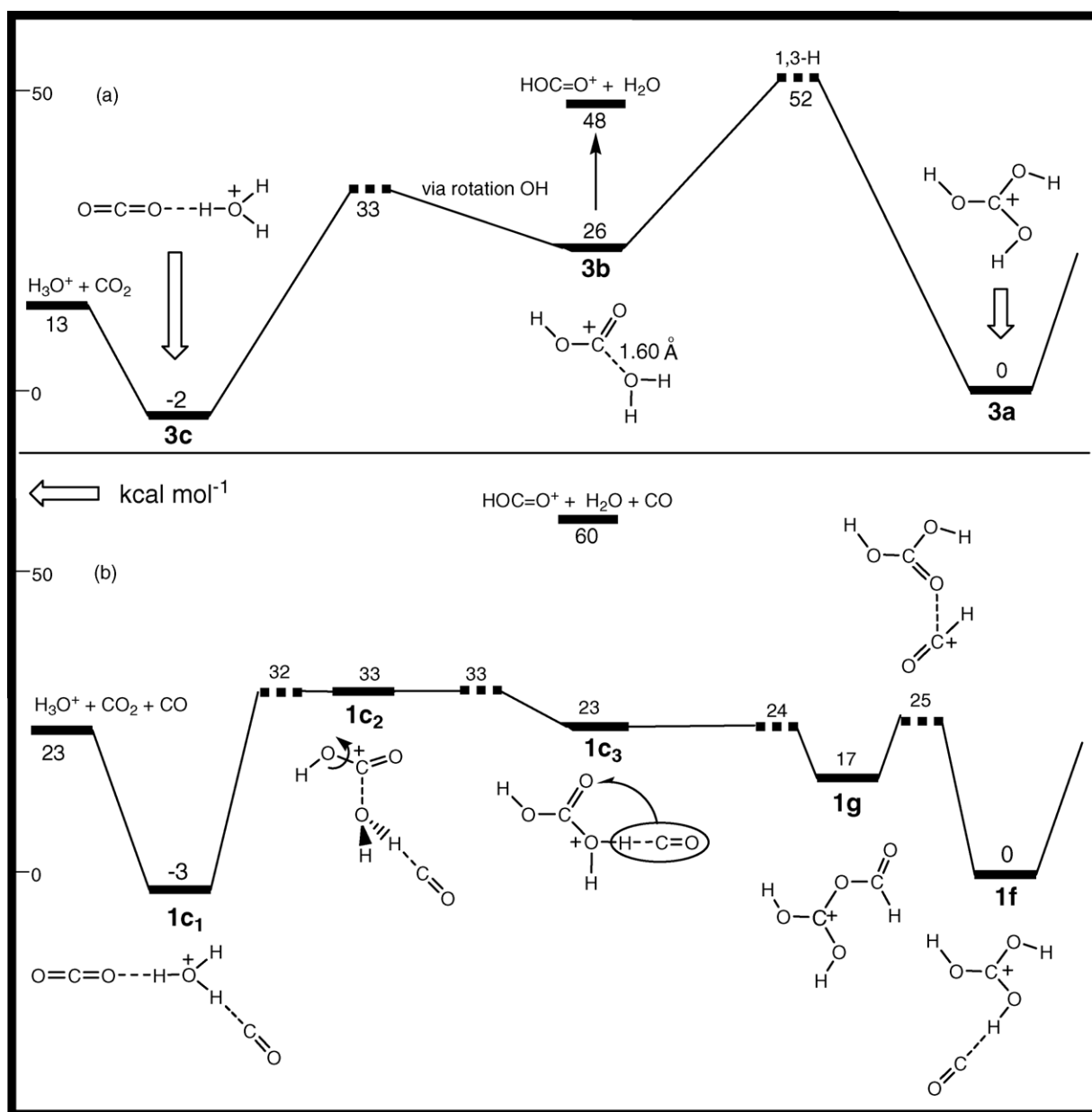


Fig. 5. Potential energy diagrams derived from CBS-QB3 calculations describing the isomerization and dissociation reactions of protonated carbonic acid isomers: (a) represents the case of solitary ions; (b) shows the effect of complexation with CO.

behind this approach is that upon neutralization the ter-body complexes will undoubtedly fall apart while the radicals $\text{HOOC}\cdot\text{C}(\text{OH})_2$ could well survive neutralization: our calculations indicate that their dissociation into $\text{HOOC-COOH} + \text{H}\cdot$ requires 29 kcal mol^{-1} . Thus, following reionization and subsequent mass selection, the MI mass spectrum of pure **1a** ions was to be recorded. Unfortunately, the yield of the survivor signal was very low; in addition the MI spectrum of m/z 91 is very weak and these two effects combined precluded a successful experiment.

We have also measured the kinetic energy releases ($T_{0.5}$ values) for the processes leading to m/z 19 (55 meV) and m/z 63 (35 meV). Now formation of m/z 63 has a larger reverse term than generation of m/z 19 (37 versus 22 kcal mol^{-1} , see

Fig. 2) and so the $T_{0.5}$ value for formation of m/z 63 should be larger than that for m/z 19 [16,17], the opposite of what is observed. Also the fraction of kinetic energy released in the formation of m/z 63, relative to the reverse term, is only 2%, an unprecedentedly low value. We therefore, propose that in the ion source a mixture of ions **1a₁** (or **1a₂**) and **1c₁** are produced. The former rearranges into energy rich **1c₁** which rapidly dissociates to H_3O^+ with a relatively large kinetic energy release and to m/z 73, $\text{O}=\text{C}=\text{O}\cdots\text{H}^+\cdots\text{CO}$. Any m/z 47 ions ($\text{H}_2\text{O}\cdots\text{H}^+\cdots\text{CO}$) and m/z 63 ions ($\text{H}_2\text{O}\cdots\text{H}^+\cdots\text{O}=\text{C}=\text{O}$) formed from **1a₁** via **1c₁** will dissociate completely to H_3O^+ . By contrast, low energy **1c₁** ions generated in the ion source produce only m/z 47 and 63 by direct bond cleavage with relatively small kinetic energy releases. Thus, the formation in

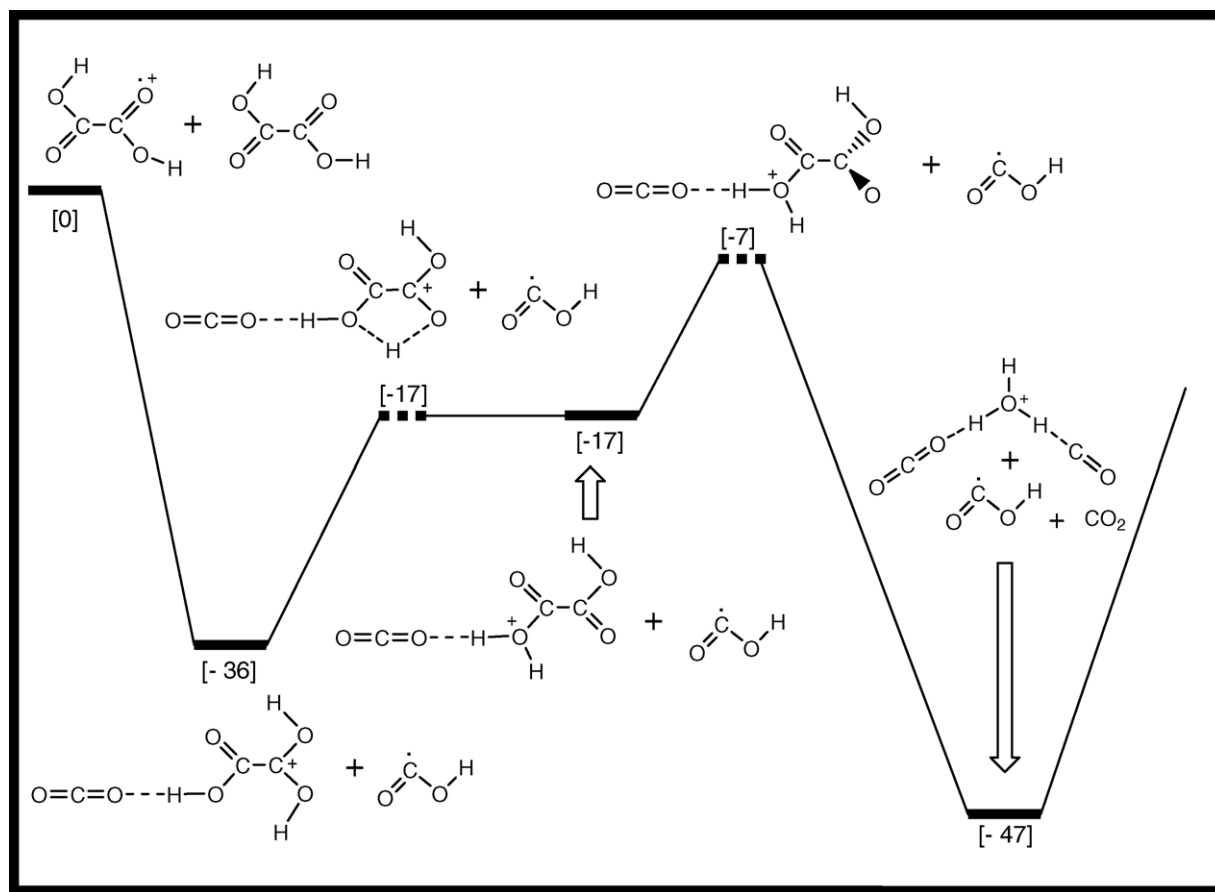


Fig. 6. Potential energy diagram derived from B3LYP/CBSB7 calculations describing the formation of the ter-body complex $\text{O}=\text{C}=\text{O}\cdots\text{H}_3\text{O}^+\cdots\text{C}=\text{O}$ from the collision encounter between neutral and ionized oxalic acid. The relative energies are in kcal mol^{-1} .

the ion source of \mathbf{Ic}_1 in admixture with \mathbf{Ia}_1 provides a rationale for the questions raised at the end of Section 3.2.

4. Summary

Protonation of oxalic acid leads to the carbenium ion $\text{HOOC-C}^+(\text{OH})_2$. Mass spectrometry based experiments reveal that this species dissociates for the major part to $\text{H}_3\text{O}^+ + \text{CO} + \text{CO}_2$, products that do not reveal the original connectivity. The mechanism of this intriguing reaction has been elucidated using the CBS-QB3 model chemistry. Key intermediate and also the reacting configuration in this rearrangement is the ter-body complex $\text{O}=\text{C}=\text{O}\cdots\text{H}_3\text{O}^+\cdots\text{CO}$, \mathbf{Ic}_1 , which can also be viewed as a hydronium bound dimer. The observed dissociation parallels that observed for neutral oxalic acid which dissociates into $\text{H}_2\text{O} + \text{CO} + \text{CO}_2$. Minor processes involve the formation of $\text{H}_2\text{O}\cdots\text{H}^+\cdots\text{CO}$, $\text{H}_2\text{O}\cdots\text{H}^+\cdots\text{O}=\text{C}=\text{O}$ and $\text{O}=\text{C}=\text{O}\cdots\text{H}^+\cdots\text{CO}$, the proton bound analogue of the ter-body complex.

Acknowledgements

JKT thanks the Natural Sciences and Engineering Research Council of Canada (NSERC) for continuing financial support. PJAR and HKE thank the Netherlands Organization for Scien-

tific Research for making available the TERAS supercomputer of SARA in Amsterdam.

References

- [1] (a) S. Yamamoto, R.A. Back, *J. Phys. Chem.* 89 (1985) 622;
(b) T. Kakumoto, K. Saito, A. Imamura, *J. Phys. Chem.* 91 (1987) 2366;
(c) J. Nieminen, M. Räsänen, J. Murto, *J. Phys. Chem.* 96 (1992) 5303;
(d) J. Higgins, X. Zhou, R. Liu, T.T.-S. Huang, *J. Phys. Chem. A* 101 (1997) 2702;
(e) C. Chen, S.-F. Shyu, *Int. J. Quantum Chem.* 76 (2000) 541.
- [2] P.C. Burgers, A.A. Mommers, J.L. Holmes, *J. Am. Chem. Soc.* 105 (1983) 5976.
- [3] H.F. van Garderen, P.J.A. Ruttink, P.C. Burgers, G.A. McGibbon, J.K. Terlouw, *Int. J. Mass Spectrom. Ion Proc.* 121 (1992) 159.
- [4] GAMESS-UK is a package of ab initio programs written by M.F. Guest, J.H. van Lenthe, J. Kendrick, K. Schoffel, P. Sherwood, with contributions from R.D. Amos, R.J. Buenker, H.J.J. van Dam, M. Dupuis, N.C. Handy, I.H. Hillier, P.J. Knowles, V. Bonacic-Koutecky, W. von Niessen, R.J. Harrison, V.R. Saunders, A.J. Stone, D.J. Tozer, and A.H. de Vries. The package is derived from the original GAMESS code due to M. Dupuis, D. Spangler, and J. Wendolowski, NRCC Software Catalogue 1, vol. 1, Program no. QG01 (GAMESS) (1980).
- [5] Gaussian 98, Revision A.9, M.J. Frisch, G.W. Trucks, H.B. Schlegel, G.E. Scuseria, M.A. Robb, J.R. Cheeseman, V.G. Zarkewski, J.A. Montgomery Jr, R.E. Stratman, J.C. Burant, S. Dapprich, J.M. Millam, A.D. Daniels, K.N. Kudin, M.C. Strain, O. Farkas, J. Tomasi, V. Barone, M. Cossi, R. Cammi, B. Mennucci, C. Pomelli, C. Adamo, S. Clifford, J. Ochterski, G.A. Petersson, P.Y. Ayala, Q. Cui, K.

- Morokuma, D.K. Malick, A.D. Rabuck, K. Raghavachari, J.B. Foresman, J. Ciolowski, J.V. Ortiz, A.G. Baboul, B.B. Stefanov, G. Liu, A. Liashenko, P. Piskorz, I. Komaromi, R. Gomperts, R.L. Martin, D.J. Fox, T. Keith, M.A. Al-Laham, C.Y. Peng, A. Nanayakkara, G. Gonzalez, M. Head-Gordon, E.S. Repogle, J.A. Pople, Gaussian Inc., Pittsburgh PA, 1998.
- [6] (a) J.A. Montgomery Jr., M.J. Frisch, J.W. Ochterski, G.A. Petersson, *J. Chem. Phys.* 110 (1999) 2822;
(b) J.A. Montgomery Jr., M.J. Frisch, J.W. Ochterski, G.A. Petersson, *J. Chem. Phys.* 112 (2000) 6532.
- [7] A. Nicolaides, A. Rauk, M.N. Glukhovtsev, L. Radom, *J. Phys. Chem.* 100 (1996) 17460.
- [8] S. Lias, J.E. Bartmess, J.F. Liebman, J.L. Holmes, R.D. Levin, W.G. Mallard, *J. Phys. Chem. Ref. Data* 17 (Suppl. 1) (1988).
- [9] See also: C. Schalley, D. Schröder, H. Schwarz, *Int. J. Mass Spectrom. Ion Proc.* 153 (1996) 173.
- [10] J. Hrusak, G.A. McGibbon, H. Schwarz, J.K. Terlouw, *Int. J. Mass Spectrom. Ion Proc.* 160 (1997) 117.
- [11] (a) G.v.d. Rest, J. Chamot-Rooke, P. Mourgues, T.B. McMahon, H.E. Audier, *J. Am. Soc. Mass Spectrom.* 12 (2001) 938;
(b) G.v.d. Rest, L.B. Jensen, A. Azeim, P. Mourgues, H.E. Audier, *J. Am. Soc. Mass Spectrom.* 15 (2004) 966.
- [12] (a) D.K. Bohme, *Int. J. Mass Spectrom. Ion Process.* 115 (1992) 95;
(b) C.Y. Wong, P.J.A. Ruttink, P.C. Burgers, J.K. Terlouw, *Chem. Phys. Lett.* 387 (2004) 204;
(c) C.Y. Wong, P.J.A. Ruttink, P.C. Burgers, J.K. Terlouw, *Chem. Phys. Lett.* 390 (2004) 176, and references cited there in.
- [13] R. Srikanth, K. Bhanuprakash, R. Srinivas, C.Y. Wong, J.K. Terlouw, *J. Mass Spectrom.* 39 (2004) 303.
- [14] J.W. Gauld, L. Radom, *J. Am. Chem. Soc.* 119 (1997) 9831.
- [15] N. Heinrich, T. Drewello, P.C. Burgers, J.C. Charles, J. Schmidt, W. Kulik, J.K. Terlouw, H. Schwarz, *J. Am. Chem. Soc.* 114 (1992) 3776.
- [16] J.L. Holmes, K. Cartledge, A.D. Osborne, *Int. J. Mass Spectrom. Ion Phys.* 29 (1979) 171.
- [17] C.J. Proctor, B. Kralj, A.G. Brenton, J.H. Beynon, *Org. Mass Spectrom.* 15 (1980) 619.